CARDIOLOGY

Mechanical circulatory support device-heart hysteretic interaction can predict left ventricular end diastolic pressure

Brian Y. Chang,[1] Steven P. Keller,[1,2]* Sonya S. Bhavsar,[3] Noam Josephy,[1,3] Elazer R. Edelman[1,4]

The full potential of mechanical circulatory systems in the treatment of cardiogenic shock is impeded by the lack of accurate measures of cardiac function to guide clinicians in determining when to initiate and how to optimally titrate support. The left ventricular end diastolic pressure (LVEDP) is an established metric of cardiac function that refers to the pressure in the left ventricle at the end of ventricular filling and immediately before ventricular contraction. In clinical practice, LVEDP is typically only inferred from, and poorly correlates with, the pulmonary capillary wedge pressure (PCWP). We leveraged the position of an indwelling percutaneous ventricular assist device and advanced data analysis methods to obtain LVEDP from the hysteretic operating metrics of the device. We validated our hysteresis-derived LVEDP measurement using mock flow loops, an animal model of cardiac dysfunction, and data from a patient in cardiogenic shock to show greater measurement precision and correlation with actual pressures than traditional inferences via PCWP. Delineation of the nonlinear relationship between device and heart adds insight into the interaction between ventricular support devices and the native heart, paving the way for continuous assessment of underlying cardiac state, metrics of cardiac function, potential closed-loop automated control, and rational design of future innovations in mechanical circulatory support systems.

INTRODUCTION

Cardiogenic shock is a critical disorder that results from inadequate end-organ perfusion after cardiac dysfunction, which manifests with severe morbidity from multiorgan system failure and mortality as high as 40% (*1*–*3*). Medical therapy for cardiogenic shock, including attempted stimulation of cardiac contractility and optimization of preload and afterload, is frequently insufficient (*4*, *5*). This has motivated the use of advanced mechanical circulatory support (MCS), such as ventricular assist devices, to enhance tissue perfusion, restore systemic homeostasis, and promote cardiac recovery (*6*–*11*).

Clinicians are challenged with determining when to initiate, maintain, wean, or advance MCS. Pulmonary artery catheters have been the traditional diagnostic tool for assessing cardiac function through the measurement of right-sided cardiac pressures, pulmonary artery oxygen tension, the thermodilution-based estimation of cardiac output, and inferred left ventricular end diastolic pressure (LVEDP) from pulmonary capillary wedge pressure (PCWP) (*12*, *13*). LVEDP, the pressure in the left ventricle at the end of ventricular filling and immediately before ventricular contraction, is elevated in cases of acute and chronic left ventricular failure, making it a useful measurement to monitor the changing clinical state of a patient (*14*, *15*). However, the information derived from pulmonary artery catheters, including PCWP measurements for LVEDP, is fraught with limitations, and increased awareness of these shortcomings has dramatically reduced use of these catheters (*16*).

Percutaneous ventricular assist devices (pVADs) positioned within the left ventricle offer not only circulatory support but also the potential of continuous direct measure of left ventricular dynamics—obviating the need for inferential measures of cardiac function. We investigated the possibility of measuring cardiac state through tracking of electromechanical controller values of an indwelling transvalvular, axial flow ventricular assist device (Impella CP). This device maintains a constant motor speed by varying motor current in response to the real-time changes in pressures in the aorta and left ventricle. We proposed using the relationship between motor current (a measure of load on the device) and pressure head (the difference between the aortic and left ventricular pressure, as defined as the pressure gradient across the pump) to derive information about the evolving physiologic state of the supported heart and imposed vascular loads. Any indwelling mechanical pump has a nominal load during steady-state operation for a given pressure head. Variable external conditions from a pulsatile heart can impose variations from the nominal load that introduce hysteresis. To maintain a fixed operating state, the pump compensates for variations by modulating motor current. Reliable measurement of motor current and aortic pressure can then provide continuous, real-time, and precise determination of a hysteresis-derived left ventricular pressure. We verified this approach in a mock circulatory loop (MCL) under simulated physiological conditions and validated the potential to provide a continuous measure of cardiac function under a variable cardiac load challenge in a porcine model. Finally, we demonstrate clinical applicability by directly comparing our hysteresis-derived LVEDP with PCWP measurements from a patient in cardiogenic shock on mechanical support.

RESULTS

Device characterization

The Impella (Abiomed), a catheter-based ventricular assist device inserted into the left ventricle across the aortic valve (Fig. 1A) to support heart function by pulling blood from the left ventricle into the aorta, served as our paradigmatic device. The system also contains an external controller console (Fig. 1B) that provides power, sets pump speed, and displays and records aortic pressure and motor current (Fig. 1C).

Pump performance curves are the traditional means of characterizing the behavior of all mechanical pumps, including those that

[1]Institute for Medical Engineering and Science, Massachusetts Institute of Technology, Cambridge, MA 02139, USA. [2]Division of Pulmonary and Critical Care Medicine, Brigham and Women's Hospital, Harvard Medical School, Boston, MA 02115, USA. [3]Abiomed Inc., Danvers, MA 01923, USA. [4]Division of Cardiology, Brigham and Women's Hospital, Harvard Medical School, Boston, MA 02115, USA.
*Corresponding author. Email: spkeller@mit.edu

are the basis of pVADs used for temporary MCS, such as the Impella (*17*–*19*). These curves depict the power required to generate a given static flow rate and pressure head (the pressure gradient across the pump). Performance curves are specific to an individual pump and are empirically determined by operating a pump at a set rotational speed [revolutions per minute (rpm)] and then varying the static pressure head while measuring the corresponding flow rate through the pump. The pump performance curve is used with the system curve, which relates the pressure head and flow characteristics of the static physical environment the mechanical pump operates in. The intersection of the two curves indicates the pump's operating point for a specific set of conditions. We used a modified representation of pump performance by showing pressure head as a function of the pump's motor current draw. The motor current acts as a surrogate for the power or load on the pump and is readily available from the Impella console.

In general, the load and power requirement of the pump at a given rpm is defined by the fluid motor torque, τ. Torque is classically defined as the product of the pressure head, *H*, and volumetric displacement per revolution, *d*.

$$\tau = H * d$$

The pump electrical power requirement ($P_{\text{electrical}}$) is, in turn, a product of the voltage (V) and current (I), and is related to the pump torque (τ), rotational speed (ω), and combined electrical and mechanical efficiency (η).

$$P_{\text{electrical}} = V * I = \frac{\tau * \omega}{\eta}$$

With a known and relatively constant motor speed and efficiency, the fluid motor torque can be determined from the electrical power of the pump. Although the relationship between power and motor current varies between pump designs, motor current is an operationally measured value for most pumps, including the Impella.

For the Impella, motor current is directly related to torque and therefore to load on the pump, here the flow rate and pressure head defined as the difference between the aortic and left ventricular pressure. Pressure head and flow are variable across the cardiac cycle with the presence of ventricular function. In this setting, the pulsatile environment causes the pump to alternate between two operating points: steady-state ventricular filling and ventricular ejection. The motor current required to generate a specific rpm is therefore dependent on dynamically changing conditions that are not present in traditional static representation of pump performance. This dynamic environment results in hysteresis, a phenomenon that occurs when system outputs are dependent on present and previous inputs (*20*), between motor current and pressure head. The resulting motor current–pressure head hysteresis loop is therefore a complete representation of the mechanical pump performance because it integrates the effects of blood flow and pressure changes from cardiac contractions with the operating properties of the pump.

Leveraging this hysteretic relationship provides the precision and premise of this work. For the Impella, variations in the load conditions arise from the dynamics of left ventricular contraction. Rather than being perceived as noise to be filtered, the motor current representing these dynamic load conditions can be used to provide insight into the underlying cardiac state. Although it had been suggested that pVAD motor current might shed light on the underlying physiologic state of the heart (*21*–*26*), the Impella allowed us to achieve such insight by harnessing cardiac hysteresis to align motor current variability over the cardiac cycle with cardiac function.

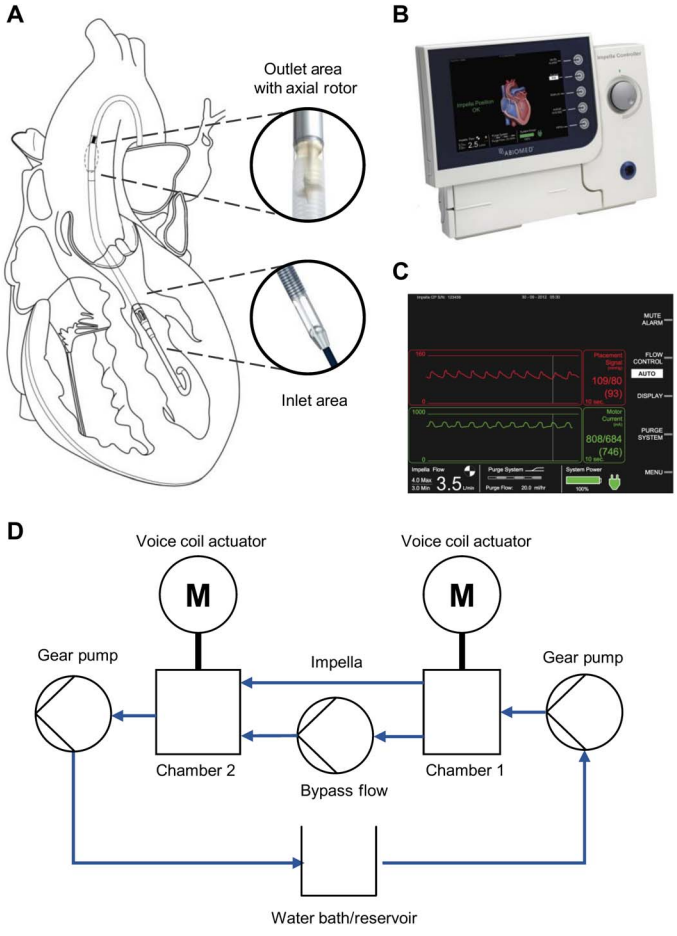

Fig. 1. Schematic of Impella placement and operation and the hybrid MCL used for initial device characterization. (**A**) The Impella, a catheter-mounted percutaneous mechanical support device that is inserted transvalvularly into the left ventricle, pulls flow from the left ventricle, across the aortic valve, and into the aorta using a mixed flow impeller. (**B**) External Impella console used to control the Impella device and record operational data, which is displayed with (**C**) an aortic pressure (red) and motor current (green). (**D**) In the MCL, the Impella is mounted between actuated pressure chambers to simulate the left ventricle (chamber 1) and aorta (chamber 2). A temperature-controlled blood-mimicking solution is circulated counterclockwise via gear pumps through the system to simulate cardiac ejection and generate pressure in the chambers. Rapid and fine pressure changes in the chambers are generated via voice coil actuators displacing metal bellows.

Mock circulatory loop

Hysteresis-derived measurement of chamber pressure using the Impella as an intraventricular MCS device was initially evaluated in an MCL (Fig. 1D). Pressures in the simulated left ventricle (chamber 1) were measured as a function of time through a single simulated cardiac contraction at different preload conditions represented by distinct LVEDP values with the same isovolumetric contraction and left ventricular ejection patterns (Fig. 2A). These varying preload states were evident in the corresponding motor current hysteresis loop, with the

point corresponding to LVEDP in each condition occurring at distinct motor current values for a given afterload (Fig. 2B). Peak systolic pressure was held constant, resulting in some variation in the slope of pressure during contraction (d*P*/d*t*).

Increasing the simulated contractility with the same preload condition produced a consistent LVEDP in the simulated left ventricle while generating a more rapid increase in the simulated rate of isovolumetric contraction (Fig. 2C). Despite the change in contractility, the point corresponding to the LVEDP in the motor current hysteresis loop did not change between the two conditions, even with markedly different shapes of the hysteresis loop through the simulated cardiac cycle (Fig. 2D).

Animal model

Once verified in the MCL, our hysteresis-derived measurement was validated in a porcine model. The left ventricular and aortic pressures were directly measured after initiation of the Impella at 37,000 rpm in an animal at baseline conditions (Fig. 3A). The measured left ventricular pressure-volume (PV) loop (Fig. 3B) and calculated pressure head plotted against the measured motor current (Fig. 3C) were defined with distinct regions to demonstrate the corresponding changes in motor current as a function of the phase of the cardiac cycle. Hysteresis manifested with markedly higher motor currents required to maintain a constant pump rotational speed during isovolumetric relaxation than during isovolumetric contraction or ejection. Moreover, a characteristic notch in the motor current hysteresis loop defined LVEDP, allowing for visual and computer-directed recognition of that point of the cardiac cycle.

The basal state was challenged through inflation of a 6- to 10-ml balloon to occlude the inferior vena cava (IVC), which evinced acute and rapid changes in LVEDP. In five different animals with an implanted Impella operating at 37,000 or 42,000 rpm, a range of baseline pressures and volumes were observed with a consistent response to the acute IVC occlusion intervention (Table 1). A total of 269 measurements of LVEDP ranged from 3.5 to 23.5 mmHg (Fig. 4A). For each animal, the hysteresis-derived LVEDP was in good agreement with the direct measurement of left ventricular pressure via indwelling Millar catheter (R^2 = 0.96; mean absolute error, 0.90 mmHg) with no clear patterns or biases in the Bland-Altman plot (Fig. 4). The case at 42,000 rpm used a different characteristic curve for hysteresis-derived LVEDP measurement but yielded similar results (R^2 = 0.96; mean absolute error, 0.84 mmHg) and trends on the Bland-Altman plot (Fig. 4).

Using data from a representative animal during the IVC occlusion (animal 1), the left ventricular PV loop obtained after the onset of IVC occlusion demonstrated a rapid decrease in left ventricular intraventricular volume followed by decreased pressure, resulting in a leftward and downward shift of the PV loop (Fig. 5A). Because the intraventricular volume decreased, the motor current hysteresis loop narrowed and shortened, reflecting a decrease in motor current variability at any given pressure head and a reduction in the pressure head across the device from the drop in systemic and intraventricular pressure. At the same time, there was a corresponding increase in motor current at the time of LVEDP (Fig. 5B).

Continuous measurements of the PCWP were obtained before and after IVC balloon inflation. PCWP measurements taken at end expiration were contrasted with the direct left ventricular catheter–measured pressures and the hysteresis-derived LVEDP (Fig. 5C). These data demonstrate marked variability in the PCWP estimates in comparison to the LVEDP values obtained by direct left ventricular catheter– and hysteresis-derived LVEDP measurements. Before IVC balloon occlusion,

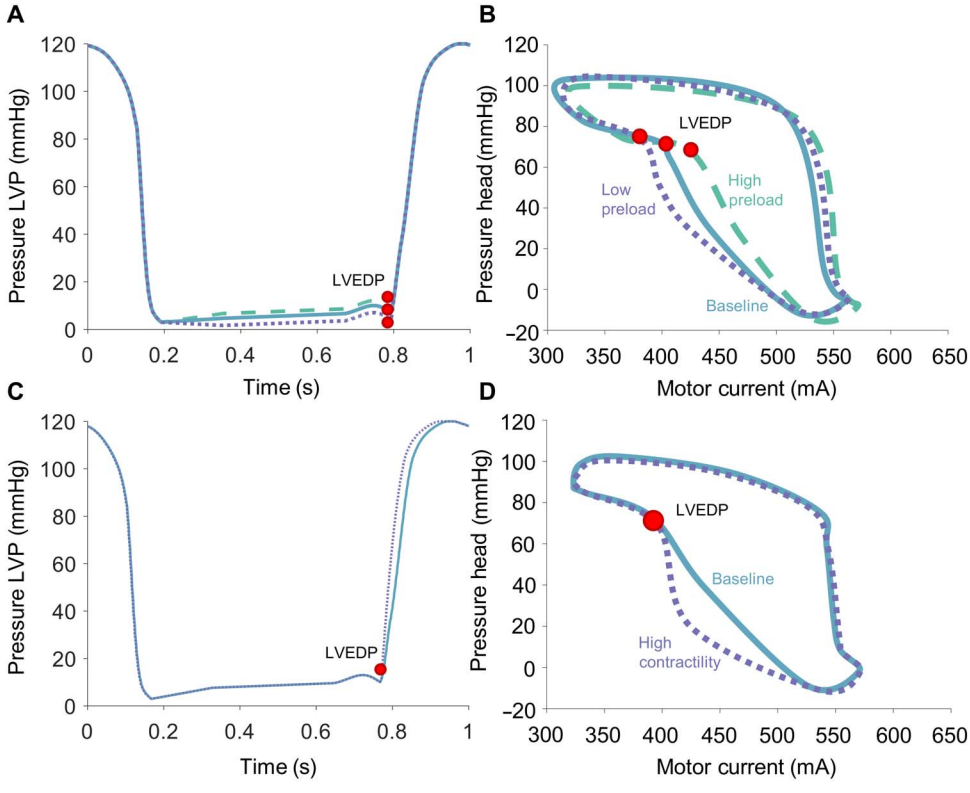

Fig. 2. Impella function in an MCL. (**A**) Varying preload conditions were tested by setting LVEDP to values including 5 mmHg (dotted), 10 mmHg (solid), and 15 mmHg (dashed), which are shown for a single representative run. Peak systolic pressure was held constant with changes in slope to accommodate different values of LVEDP (red dot). (**B**) In a representative case with Impella speed of 37,000 rpm, LVEDP (red dot) is located at different points on the motor current hysteresis loop with each condition. (**C**) Left ventricular pressure (LVP) tracings with different slopes of systolic contraction (d*P*/d*t*) were used to simulate varying contractility from 1100 mmHg/s (solid) to 1600 mmHg/s (dotted). LVEDP (red dot) is held constant. (**D**) In a representative case with Impella speed of 37,000 rpm, LVEDP (red dot) does not change with variable contractility.

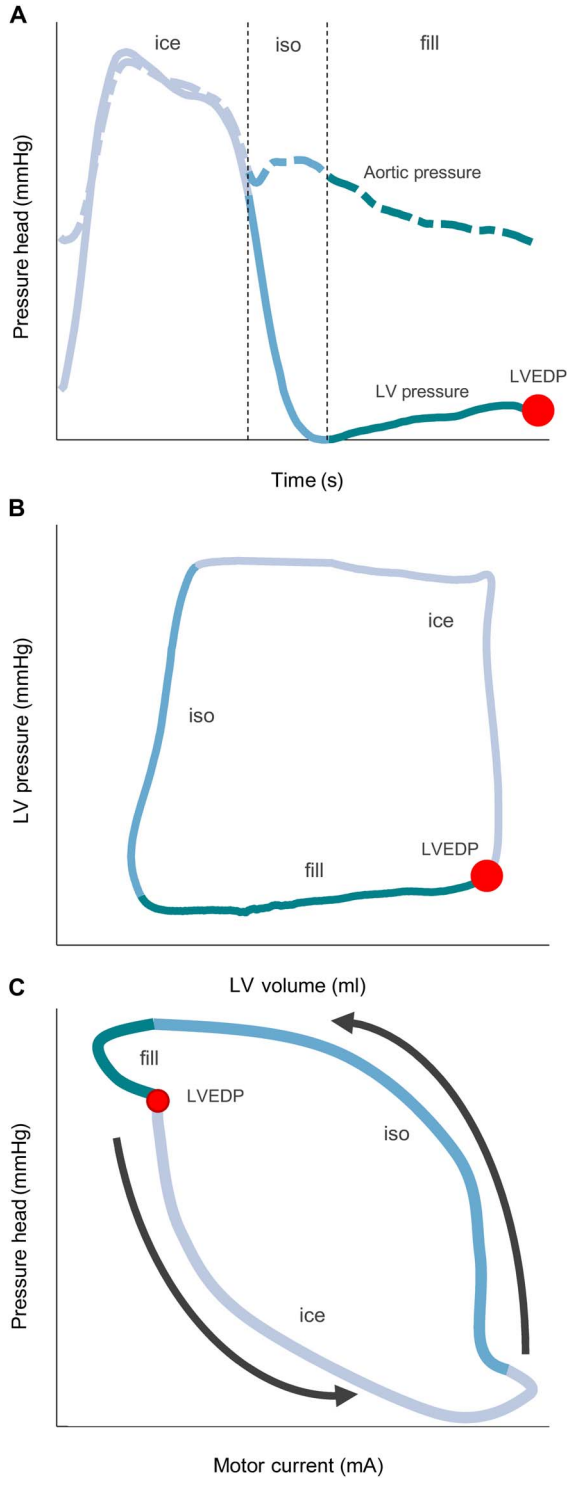

Fig. 3. The cardiac cycle separated into phases of ventricular isovolumetric contraction and ejection (ice), isovolumetric relaxation (iso), and diastolic filling (fill). (**A**) Left ventricular (LV) (solid line) and aortic (dashed line) pressures over time, (**B**) left ventricular PV loop corresponding to the time series in (A), and (**C**) motor current hysteresis loop corresponding to the same heart beat as (A) and (B). This hysteresis loop can be separated into these different phases and cycles in a counterclockwise direction as indicated by the arrows. Phase separation allows easier determination of various effects on the loop from changing cardiac state. LVEDP is indicated in all panels by a red dot.

the PCWP registered a value of 9.7 ± 2.7 mmHg, whereas direct measurement of LVEDP was 17.4 ± 1.1 mmHg and hysteresis-derived measurement of LVEDP was 17.5 ± 1.2 mmHg, an almost fivefold greater error in the PCWP than the hysteresis-derived measures. After IVC balloon occlusion, the calculated LVEDP values tracked closely to the directly measured values (mean absolute error, 0.9 mmHg), whereas the measured PCWP demonstrated continued variability (mean absolute error, 5.8 mmHg).

Patient data

We applied the hysteresis-derived LVEDP measurement to data from a patient supported on an Impella placed in the setting of cardiogenic shock. The respiratory cycle induces not only physiologic variation in ventricular filling and LVEDP (Fig. 6A) but also respirophasic error in PCWP from cyclical alveolar compression of pulmonary capillaries. Breath hold reduces compression by the filled alveolae of pulmonary vasculature, but can be difficult to perform in every patient. At a time point with a chart report value of 14 mmHg, hysteresis-derived LVEDP was 18.9 ± 2.6 mmHg (n = 25; Fig. 6A). The mean absolute difference of 5.2 mmHg between the hysteresis-derived measurement and PCWP was similar to that found in our animal study. At a second time point, a PCWP waveform was recorded during a breath hold that yielded a mean of 33.7 ± 2.9 mmHg with a hysteresis-derived LVEDP measurement of 30.7 ± 2.5 mmHg (n = 6 samples; Fig. 6B). This resulted in a mean absolute difference of 2.8 mmHg between the hysteresis-derived measurement and PCWP.

DISCUSSION

Cardiogenic shock is a highly morbid condition that frequently fails to respond to optimal medical therapy. There is an increasing interest in use and prompt initiation of MCS support to restore systemic homeostasis (*27*–*29*). However, it is difficult for a clinician to determine when to initiate, how to optimally titrate, and when to withdraw mechanical support especially because no firm metrics of support and clinical benefit exist. Guidance is limited to qualitative assessment or indirect estimates of left ventricular function, such as PCWP. Using the PCWP to determine LVEDP is limited to the time over which balloon inflation can be performed and is prone to significant error from pressure tracing noise contamination and variability (*12*, *13*, *30*). In studies of patients with both pulmonary artery catheters and methods of direct measurements of left ventricular pressure, the PCWP can deviate from the LVEDP by more than 6 mmHg (*12*, *13*, *31*). Our data confirm this value with a mean absolute error of 5.8 mmHg. The presence of a device in the left ventricle offers the opportunity to respond to this challenge with far greater fidelity. These devices modulate their motor current to respond to demands of load and cardiac state, thereby providing the means to track cardiac function through interactions between the indwelling pVAD and the supported heart.

Unlike traditional pump operating environments, the pVAD functions in a highly dynamic environment due to cardiac contractions. The Impella pVAD operates in this environment by providing variable motor current to the pump to maintain a constant rpm. The Impella is ideal for our application because it can be placed into the heart without damage to the organ, resides within the left ventricle to provide physiologic-like antegrade flow from the left ventricle into the aorta, and has a fixed cannula length with standardized positioning and a small impeller mass relative to the mass flow. The motor current required to maintain a set rotational speed varies during the cardiac

Table 1. Basic hemodynamics for each animal case at baseline and during intervention. Each animal trial was performed independently in five pigs using the IVC occlusion intervention. An additional case was performed with animal 5 at a different operating speed (42K = 42,000 rpm) to demonstrate parity at multiple speeds. ΔP is the pressure difference between the aortic and left ventricular pressure, of which all animals had a minimum gradient of ~0 mmHg. Mean arterial pressure (MAP) is shown at baseline and during peak intervention. bpm, beats per minute.

	Animal 1	Animal 2	Animal 3	Animal 4	Animal 5	Animal 5 (42K)
Mass (kg)	77.3	70.0	79.4	71.4	68.0	68.0
Heart rate (bpm)	125	110	97	116	129	110
MAP baseline (mmHg)	104.0	65.3	88.1	83.3	98.2	98.6
MAP occlusion (mmHg)	71.8	38.2	71.7	62.1	60.5	79.5
ΔP max (mean) (mmHg)	109.0 (41.9)	70.2 (21.9)	105.4 (45.7)	93.4 (33.7)	81.3 (32.1)	90.9 (38.3)
LVEDP max/min (mean) (mmHg)	19.5/4.4 (15.8)	9.4/3.1 (8.4)	7.1/4.7 (6.0)	13.8/10.1 (12.3)	23.5/15 (22)	23.8/9.0 (19.7)
LVEDP data points	45	62	35	33	94	32
Mean absolute error (mmHg)	0.92	0.31	1.58	0.98	1.00	0.84

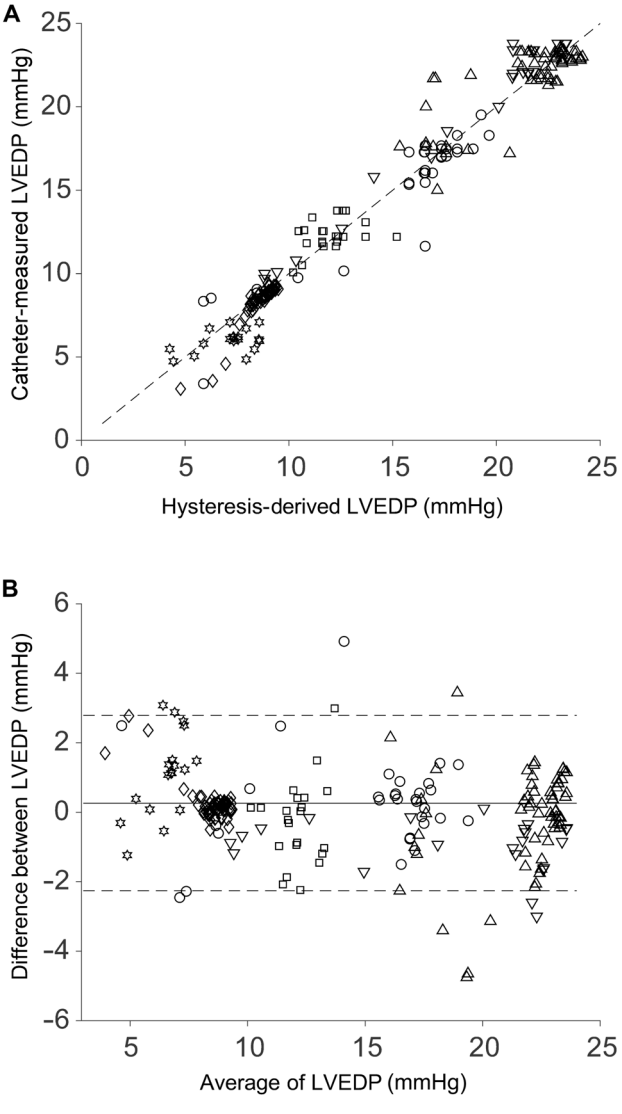

Fig. 4. Accuracy of hysteresis-derived measurement compared to direct indwelling catheter measurement over multiple animal trials. Data from five pigs with an implanted Impella operating at 37,000 or 42,000 rpm had varying baseline LVEDP values and effect size from an IVC occlusion. Each point (n = 269) represents a separate measurement comparison, and each marker represents a different case (Table 1), with the 42,000 rpm represented by the downward triangle. (**A**) Correlation plot comparing hysteresis-derived and directly measured LVEDP (R^2 = 0.96) for all animals, with the dashed line representing the unity correlation. (**B**) Bland-Altman plot for all animals with standard confidence intervals using ±2 SDs of the difference between the hysteresis-derived and directly measured LVEDP over the average result of both methods.

cycle, with the degree of variation dependent on the underlying physiologic state of the heart. The impact of the contracting heart on the device performance produces a characteristic hysteresis loop.

Verification and physiologic validation

Experiments conducted in the MCL allowed us to assess the impact of changes in specific parameters of cardiac function, such as the preload and the contractility, on the pump head–motor current hysteresis loop. The data presented demonstrate that the shape of the hysteresis loop changes with preload and contractility in a way that can distinguish the type of change occurring. For example, the effect of varying LVEDP versus change in contractility (dP/dt) can be distinguished by comparing the preload variation case with the isolated contractility change case. Furthermore, LVEDP can be readily extracted from the hysteresis loop morphology because it appears as an inflection point when the pump changes from encountering a left ventricle undergoing diastolic filling with one that is actively contracting. The inflection point was observed in both the MCL and animal experiments, and shown in the MCL to be independent of varying contractility state.

Validation was performed using physiologically intact animal models with controlled alteration and restoration of ventricular input (volume) through IVC occlusion. IVC occlusion is the classic means by which to cause controlled, graded changes in LVEDP over a wide range, and allows for internal control and validation with return to baseline without irreversible pathologic insult. The hysteresis-derived LVEDP measured from animal data derived from the Impella resulted

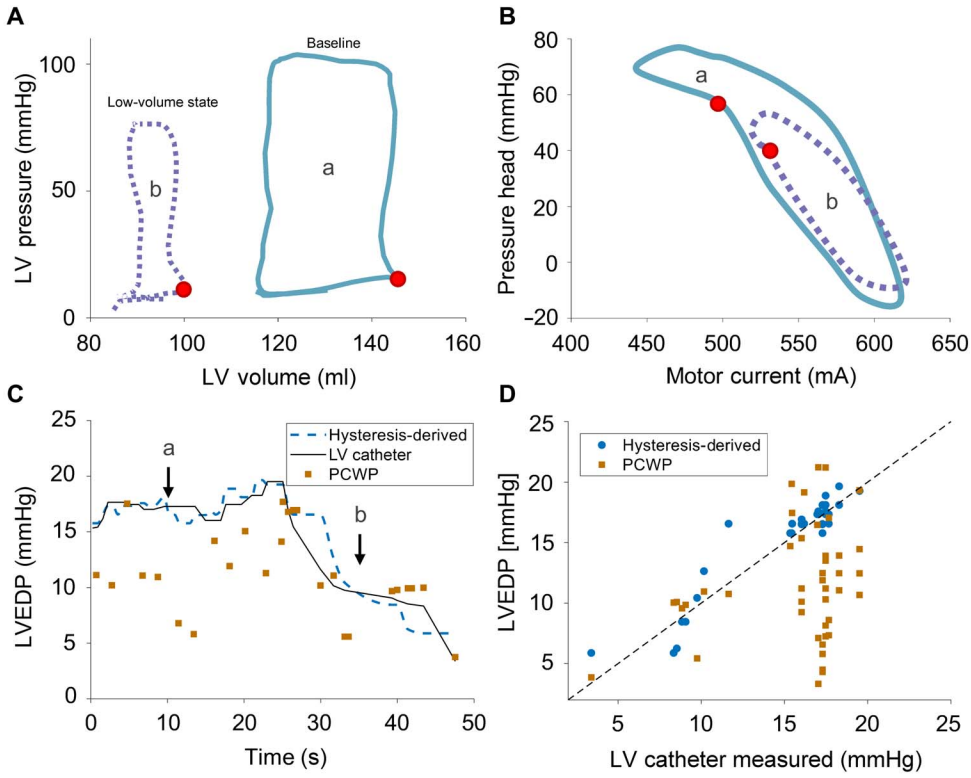

Fig. 5. LVEDP measurement during IVC occlusion. Hemodynamics at baseline (a, solid blue line) and during IVC occlusion before Impella suction event (b, dotted purple line). (**A**) Left ventricular PV loops from Millar catheter demonstrate reduction in end diastolic pressure and stroke volume. (**B**) Hysteresis loops exhibit increased motor current during diastolic filling and a shift in notch (red dot) corresponding to end diastolic pressure from the effects of the IVC occlusion. (**C**) LVEDP over time via hysteresis-derived method (dashed blue line), direct catheter (solid black line), and PCWP measurement (orange square). (**D**) Correlation plot of the hysteresis-derived (blue circle; $R^2 = 0.88$) and PCWP (orange square; $R^2 = 0.04$) measurements to direct measurement of LVEDP, with the dashed black line representing the unity correlation.

in a value that tracked closely with the direct measurement of LVEDP through an indwelling catheter in the animal ventricle with a correlation of $R^2 = 0.96$. Hysteresis-derived LVEDP was fivefold more accurate than PCWP measurements in our animals, matching data reported in the literature using similar techniques (*12*, *13*, *31*). Moreover, the hysteresis-derived measurement tracked changes in LVEDP with respiratory variation and changes induced by the IVC occlusion at a higher resolution than achievable with the PCWP.

The change in the shape of the pressure head–motor current hysteresis loop with changing conditions evaluated in the MCL and the animal model suggests that the use of the hysteresis loop could provide insight into other predictors of cardiac state. The width of the hysteresis loop increased in the MCL high contractility state compared with the baseline condition, whereas the animal model of acute disease demonstrated a decreased width of the hysteresis. The change in width seen in the MCL and animals is indicative of the inertial change that occurs with varying contractile force of the heart. The additional hysteresis loop changes in the animal are due to change in pressure head from reduced ejection related to the Frank-Starling mechanism, which cannot be controlled in the intact physiologic model. Imaginative quantification of the hysteresis loop can lead to new means to describe cardiac state and is being investigated.

The patient data analysis suggests clinical applicability and validity of the hysteresis-derived LVEDP measurement. With normal respiratory variation, patient chart–reported PCWP and hysteresis-derived measurement were comparable with animal data results and previous studies; PCWP was lower than the hysteresis-derived LVEDP and had a similar mean absolute difference (5.2 mmHg versus 5.8 mmHg) (*12*, *13*, *31*). Because error in PCWP is sensitive to respiratory effects (*31*), comparison was also evaluated with a patient during an end-expiratory breath hold. When using a full PCWP waveform during the end-expiratory breath hold, it is evident that PCWP maintains increased variability compared to the hysteresis-derived LVEDP measurement, but with reduced mean absolute difference. The reduction in mean absolute difference when comparing both hysteresis-derived measurements during an end-expiratory breath hold versus standard PCWP readings was nearly 3 mmHg, which is similar to a previous study comparing the error of traditional readouts of PCWP to end-expiratory measurements (*31*). Although PCWP remains sensitive to the pressure changes induced by respiratory variation, these results suggest that the hysteresis-derived measurement remains robust with the respiratory cycle. The trends and patterns of these differences in measurements suggest some internal consistency when comparing PCWP with the hysteresis-derived measurement and provide indication of the applicability of this method in a clinical setting.

Limitations and future work

Although the analysis of the hysteresis loop using motor current is shown to be useful, there are some limitations to the work in its current form. LVEDP is relatively predictable with characterization; however, the use of the entire hysteresis loop as a method to track cardiac function requires more extensive characterization. Determination of LVEDP is also dependent on data sampling rate. Because LVEDP and many other features of the cardiac cycle refer to specific areas of the cardiac cycle, they may not be captured if the sampling rate is overwhelmed by more rapid heart rates. This sampling constraint is resolved by measuring over multiple beats; because more points are accumulated, natural physiologic variation between beats prevents isorhythmic repeated loss of the LVEDP. Sensitivity analysis determined that a time window of 5 s would result in LVEDP being captured 93% of the time for heart rates up to 300 bpm. In addition, although several animals have been challenged with large and sudden changes in pressure, further studies must consider chronic changes and potential adaptive reflexes to understand how our approach might operate over longer terms and in the face of device variability. The current use of patient data illustrates that the technology can be used with the current clinical setting, but

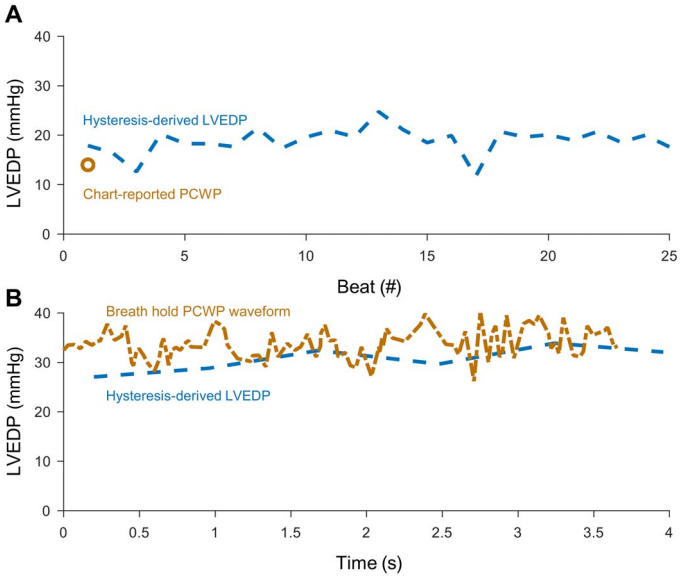

Fig. 6. LVEDP measurement from retrospective patient data. Data are shown around discrete time points with available PCWP data. (**A**) A patient chart–extracted PCWP estimation (orange circle) for LVEDP is compared with the hysteresis-derived LVEDP (dashed blue line) for 25 heart beats. (**B**) A separate time point with a digitized waveform of PCWP (dashed-dotted orange line) during a breath hold and the hysteresis-derived LVEDP (dashed blue line).

further study of patient data in a larger number of patients will be necessary to demonstrate clinical efficacy.

The full potential of temporary mechanical support during acute cardiogenic disease has yet to be realized because of the difficulty in determining appropriate degree of support, especially with the goal of promoting native heart recovery. A modified hysteresis loop comparing the pressure head, as the difference between the aortic and left ventricular pressure, to the device motor current, as a measure of load on the device, can help alleviate this problem by characterizing the device-heart interaction. By using parameters already measured by the device, the loop can be used to quantitatively and visually provide information about the state of the heart, which, in turn, can be used to provide guidance on appropriate degree of support. Here, we have shown that the motor current–pressure head relationship can be used to determine LVEDP. Comparison with PCWP and a direct catheter measurement of the LVEDP provides a contextual view of a future wherein mechanical support devices can provide continuous functional metrics of cardiac state and ultimately closed-loop feedback control and titration.

MATERIALS AND METHODS

Study design

The goal of this work was to develop and evaluate a method to use MCS device operational signals to determine LVEDP. Devices were characterized in an MCL, validated using a porcine animal model via direct left ventricular pressure and PCWP measurement, and applied using clinically available data through retrospective patient data analysis. MCL experiments were used to evaluate characteristics of each device used in an animal study over the widest clinically applicable range of LVEDP. Such characterization was applied to five different animals during baseline and during IVC occlusion intervention. This intervention was chosen because of the controlled, rapid, and large changes it induces in LVEDP and hemodynamic state of the animal. Retrospective patient data were collected on the basis of available patients with hemodynamic measurements for validation.

Impella CP

The Impella CP served as our paradigmatic model of a pVAD. The Impella is a temporary percutaneous, transvalvular MCS device that resides within the left ventricle and maintains a constant pump speed through load sensing. A continuous mixed flow pump at the end of a 9-French catheter (*32*) is threaded percutaneously retrograde through the aorta across the aortic valve into the left ventricle via either the femoral or axillary artery. The inlet area of the catheter is in the left ventricle, and the outlet area, where the impeller and motor are located, lies in the aorta (Fig. 1A). The distal end of the device connects to a controller console (Fig. 1B) that records motor current, motor speed, and aortic pressure (Fig. 1C). The console sends power and the fixed rotor speed setting to the device. Power is controlled using pulse-width modulation, which allows direct relation of power to motor current, to maintain a fixed rpm setting even in the face of rapidly changing operating environment and cardiac function.

Mock circulatory loop

Variations in the pressure head and motor current relationship were investigated using simulated cardiac states in a previously qualified hybrid MCL (*33*) that consists of two chambers, two voice coil actuators (one per chamber), three gear pumps, a fluid bath, controllers for each component, and a computer controller (Fig. 1D). Flow was drawn from a fluid bath by a gear pump into chamber 1, which simulated the left ventricle, and flowed counterclockwise into chamber 2, which simulated the aorta. Flow moved from chamber 1 to chamber 2 either through a bypass flow path (native aortic ejection) or through a fixture that was tightly sealed around the Impella (pump flow). Flow then exited chamber 2 and returned to the fluid bath to model systemic circulation. Each actuator was controlled in real time using custom controllers and a CAN bus connection to a computer running a custom LabVIEW program (National Instruments).

Desired custom pressure waveforms for both the simulated left ventricle and aorta were input via the LabVIEW program, and output values were saved on the computer. The gear pumps introduced circulating fluid to generate the programmed pressure, which was then precisely and rapidly controlled by the voice coil actuators for each chamber (± 1 mmHg) (*33*). The voice coil actuators moved linearly to change the effective chamber volumes through expanding and contracting metal bellows.

To mimic blood rheology, the circulating fluid consisted of distilled water with 33% glycerol, 0.2% sodium hypochloride, and 0.01% silver by mass maintained at 37°C. The chamber 1 pressure waveform had a nominal LVEDP of 10 mmHg with values that varied from 5 to 45 mmHg. The pressure waveform in chamber 2 had a nominal end diastolic pressure of 80 mmHg with values that varied from 30 to 130 mmHg. The resulting pressure head values ranged from 20 to 120 mmHg depending on Impella speed—higher speeds allow greater pressure heads without retrograde flow. Changes in cardiac contractility were simulated using a variation in the slope of pressure during contraction (dP/dt), with 1100 mmHg/s used as the baseline contractility and 1600 mmHg/s used as a high contractility state. A pressure transducer near the inlet of the Impella was used to report the simulated left ventricular pressure. Data from the MCL were analyzed using MATLAB (MathWorks).

Hysteresis-derived LVEDP

LVEDP is the pressure in the left ventricle at the end of ventricular filling and immediately before ventricular contraction. The relationship between the contractile state of the heart and LVEDP is described by the Frank-Starling relationship. Because LVEDP is elevated in cases of acute and chronic left ventricular failure, monitoring trends in LVEDP can provide insights into the changing clinical state of a patient (*14*, *15*). Given the clinical importance of the measurement of LVEDP, we developed a method to measure LVEDP by using the motor current–pressure head relationship.

Motor current and the pressure head that corresponded to LVEDP over the different hemodynamic states were recorded at a given rpm. We assumed that motor current variations stemming from slight motor speed deviations at end diastole were relatively linear and were thus corrected by linear scaling to the ideal fixed motor speed as follows:

$$i_c = i_m * \frac{\omega_0}{\omega}$$

in which the speed-corrected motor current (i_c) is equal to the product of the measured motor current (i_m) and a ratio of the desired fixed (ω_0) and real (ω)motor speeds. This correction is made because deviations in motor speed arise from controller variance rather than change in physiologic state. Without correction, motor speed variance can result in falsely inconsistent motor current for a given physiologic state. The speed-corrected motor current (i_c) was plotted against the measured pressure head for at least eight different conditions in the MCL, and the relationship was then fit using an R^2 optimization to produce a third-order polynomial with pressure head as a function of motor current. Coefficients for the fit were used to determine LVEDP from a given corrected motor current at a given motor rpm setting.

Animal model

A swine model served to provide insight into performance of the hysteresis-derived LVEDP measurement in an intact living system at baseline and after acute interventions via mechanical occlusion of venous return. Five (73.2 ± 4.9 kg; Table 1) Yorkshire swine were sedated with an intramuscular injection of Telazol (tiletamine and zolazepam; Zoetis US) at 6 mg/kg, endotracheally intubated, and maintained under general anesthesia with inhaled isoflurane. Animals were maintained in accordance with National Institutes of Health (NIH) and Association for Assessment and Accreditation of Laboratory Animal Care (AAALAC) guidelines (CBSET) and monitored by continuous recording of oxygen saturation, core body temperature, and three-lead electrocardiogram.

Arterial and venous access was obtained via cutdown of the left and right femoral arteries and veins and right jugular vein. A pulmonary artery catheter was introduced via the jugular vein to the pulmonary artery for measurement of the PCWP. The Impella was introduced via the left femoral artery over wire into the left ventricle using fluoroscopy guidance. A pigtail-tipped conductance PV loop catheter (Millar) was introduced via the right femoral artery and advanced into the left ventricle parallel to the Impella for continuous measurement of the left ventricular volume and pressure. Ultrasound and fluoroscopy were used to guide and confirm placement of the Impella and catheters. The Impella was operated at the 37,000 or 42,000 rpm setting, which are the intermediate and highest setting for therapeutic use (*32*), with continuous measurement of motor speed, motor current, and aortic pressure.

To model an acute and rapid change in LVEDP, a catheter-based balloon was inserted into the femoral vein and advanced to the IVC at the level of the diaphragm and inflated to occlude, thus causing a rapid preload change in the heart. Pharmaceutical interventions have not been as effective in creating predictable and well-controlled changes in hemodynamics, especially in the setting of MCS. The IVC balloon was maintained at full inflation until an Impella console–reported suction event occurred. Because the device and hysteresis-derived LVEDP measurement rely only on hemodynamic state, rather than pathophysiology, the IVC occlusion intervention is a good model to stress the hysteresis-derived measurement with an acute and controlled rapid change in LVEDP. Data were registered and analyzed using MATLAB. All experimental procedures and protocols followed NIH and institutional guidelines regarding humane care and use of laboratory animals.

Patient data

Anonymized retrospective patient data were obtained to provide further validation and demonstrate clinical applicability in uncontrolled environments. Retrospective data from a patient suffering acute cardiogenic shock treated using Impella CP were provided by Brigham and Women's Hospital as per institutional review board policy. The PCWP value and waveform tracings were obtained when available for comparison with calculated LVEDP value. Values were extracted from review of the patient chart. Waveform tracings were digitized using custom MATLAB scripts. Other information about the clinical course was provided via consultation with a treating attending physician.

This clinical information was coupled with Impella console data routinely downloaded post-Impella explant, which included placement signal, motor current, and pump speed. These were used with the same hysteresis-derived LVEDP measurement as used in the animal models at discrete time points, where clinical information was available. Time periods for LVEDP calculation are limited by available hemodynamic data for validation.

Statistical analysis

Bland-Altman and correlation plots using ±2 SD confidence intervals were used with animal data to assess validity of the measurement technique with other measurement standards (*34*). A coefficient of determination is calculated to compare the linear correlation between techniques. Animal and patient results at specific states are expressed as means ±SD, with differences between techniques calculated using the mean absolute error. Statistical analysis was conducted using MATLAB and the Statistics and Machine Learning Toolbox from MATLAB.

REFERENCES AND NOTES

1. D. Mozaffarian, E. J. Benjamin, A. S. Go, D. K. Arnett, M. J. Blaha, M. Cushman, S. R. Das, S. de Ferranti, J. P. Després, H. J. Fullerton, V. J. Howard, M. D. Huffman, C. R. Isasi, M. C. Jiménez, S. E. Judd, B. M. Kissela, J. H. Lichtman, L. D. Lisabeth, S. Liu, R. H. Mackey, D. J. Magid, D. K. McGuire, E. R. Mohler III, C. S. Moy, P. Muntner, M. E. Mussolino, K. Nasir, R. W. Neumar, G. Nichol, L. Palaniappan, D. K. Pandey, M. J. Reeves, C. J. Rodriguez, W. Rosamond, P. D. Sorlie, J. Stein, A. Towfighi, T. N. Turan, S. S. Virani, D. Woo, R. W. Yeh, M. B. Turner; American Heart Association Statistics Committee and Stroke Statistics Subcommittee, Heart disease and stroke statistics—2016 update: A report from the American Heart Association. *Circulation* **133**, e38–e360 (2016).
2. P. A. Heidenreich, J. G. Trogdon, O. A. Khavjou, J. Butler, K. Dracup, M. D. Ezekowitz, E. A. Finkelstein, Y. Hong, S. C. Johnston, A. Khera, D. M. Lloyd-Jones, S. A. Nelson, G. Nichol, D. Orenstein, P. W. F. Wilson, Y. J. Woo, Forecasting the future of cardiovascular disease in the United States: A policy statement from the American Heart Association. *Circulation* **123**, 933–944 (2011).

3. V. L. Roger, Epidemiology of heart failure. *Circ. Res.* **113**, 646–659 (2013).
4. A. Reyentovich, M. H. Barghash, J. S. Hochman, Management of refractory cardiogenic shock. *Nat. Rev. Cardiol.* **13**, 481–492 (2016).
5. L. De Luca, Z. Olivari, A. Farina, L. Gonzini, D. Lucci, A. Di Chiara, G. Casella, F. Chiarella, A. Boccanelli, G. Di Pasquale, S. De Servi, F. M. Bovenzi, M. M. Gulizia, S. Savonitto, Temporal trends in the epidemiology, management, and outcome of patients with cardiogenic shock complicating acute coronary syndromes. *Eur. J. Heart Fail.* **17**, 1124–1132 (2015).
6. M. M. Givertz, Ventricular assist devices: Important information for patients and families. *Circulation* **124**, e305–e311 (2011).
7. W. Tayara, R. C. Starling, M. H. Yamani, O. Wazni, F. Jubran, N. Smedira, Improved survival after acute myocardial infarction complicated by cardiogenic shock with circulatory support and transplantation: Comparing aggressive intervention with conservative treatment. *J. Heart Lung Transplant.* **25**, 504–509 (2006).
8. C. S. Rihal, S. S. Naidu, M. M. Givertz, W. Y. Szeto, J. A. Burke, N. K. Kapur, M. Kern, K. N. Garratt, J. A. Goldstein, V. Dimas, T. Tu; Society for Cardiovascular Angiography and Interventions (SCAI); Heart Failure Society of America (HFSA); Society of Thoracic Surgeons (STS); American Heart Association (AHA); American College of Cardiology (ACC), 2015 SCAI/ACC/HFSA/STS Clinical Expert Consensus Statement on the Use of Percutaneous Mechanical Circulatory Support Devices in Cardiovascular Care (Endorsed by the American Heart Association, the Cardiological Society of India, and Sociedad Latino Americana de Cardiologia Intervencion; Affirmation of Value by the Canadian Association of Interventional Cardiology–Association Canadienne de Cardiologie d'intervention). *J. Cardiac Fail.* **21**, 499–518 (2015).
9. B. Meyns, J. Stolinski, V. Leunens, E. Verbeken, W. Flameng, Left ventricular support by Catheter-Mountedaxial flow pump reduces infarct size. *J. Am. Coll. Cardiol.* **41**, 1087–1095 (2003).
10. M. Dandel, R. Hetzer, Myocardial recovery during mechanical circulatory support: Weaning and explantation criteria. *Heart Lung Vessel.* **7**, 280–288 (2015).
11. M. Dandel, R. Hetzer, Myocardial recovery during mechanical circulatory support: Long-term outcome and elective ventricular assist device implantation to promote recovery as a treatment goal. *Heart Lung Vessel.* **7**, 289–296 (2015).
12. P. E. Marik, Obituary: Pulmonary artery catheter 1970 to 2013. *Ann. Intensive Care* **3**, 38 (2013).
13. T. J. Iberti, E. P. Fischer, A. B. Leibowitz, E. A. Panacek, J. H. Silverstein, T. E. Albertson, A multicenter study of physicians' knowledge of the pulmonary artery catheter. *JAMA* **264**, 2928–2932 (1990).
14. P. Hamosh, J. N. Cohn, Left ventricular function in acute myocardial infarction. *J. Clin. Invest.* **50**, 523–533 (1971).
15. J. S. Forrester, G. Diamond, T. J. McHugh, H. J. C. Swan, Filling pressures in the right and left sides of the heart in acute myocardial infarction—A reappraisal of central-venous-pressure monitoring. *N. Engl. J. Med.* **285**, 190–193 (1971).
16. K. Ikuta, Y. Wang, A. Robinson, T. Ahmad, H. M. Krumholz, N. R. Desai, National trends in use and outcomes of pulmonary artery catheters among Medicare beneficiaries, 1999-2013. *JAMA Cardiol.* **2**, 908–913 (2017).
17. F. Moscato, G. A. Danieli, H. Schima, Dynamic modeling and identification of an axial flow ventricular assist device. *Int. J. Artif. Organs* **32**, 336–343 (2009).
18. P. Naiyanetr, F. Moscato, M. Vollkron, D. Zimpfer, G. Wieselthaler, H. Schima, Continuous assessment of cardiac function during rotary blood pump support: A contractility index derived from pump flow. *J. Heart Lung Transplant.* **29**, 37–44 (2010).
19. H. Schima, H. Boehm, L. Huber, H. Schmallegger, M. Vollkron, M. Hiesmayr, R. Noisser, G. Wieselthaler, Automatic system for noninvasive blood pressure determination in rotary pump recipients. *Artif. Organs* **28**, 451–457 (2004).
20. I. D. Mayergoyz, *Mathematical Models of Hysteresis and Their Applications* (Academic Press, ed. 2, 2003).
21. K. Ohuchi, D. Kikugawa, K. Takahashi, M. Uemura, M. Nakamura, T. Murakami, T. Sakamoto, S. Takatani, Control strategy for rotary blood pumps. *Artif. Organs* **25**, 366–370 (2001).
22. M. Oshikawa, K. Araki, G. Endo, H. Anai, M. Sato, Sensorless controlling method for a continuous flow left ventricular assist device. *Artif. Organs* **24**, 600–605 (2000).
23. T. Tsukiya, T. Akamatsu, K. Nishimura, T. Yamada, T. Nakazeki, Use of motor current in flow rate measurement for the magnetically suspended centrifugal blood pump. *Artif. Organs* **21**, 396–401 (1997).
24. G. Endo, K. Araki, K. Kojima, K. Nakamura, Y. Matsuzaki, T. Onitsuka, The index of motor current amplitude has feasibility in control for continuous flow pumps and evaluation of left ventricular function. *Artif. Organs* **25**, 697–702 (2001).
25. L. A. Baloa, D. Liu, J. R. Boston, M. A. Simaan, J. F. Antaki, Control of rotary heart assist devices, *Proceedings of the 2000 American Control Conference*, Chicago, IL, 28 to 30 June 2000 (IEEE, 2002).
26. L. Fresiello, F. Rademakers, P. Claus, G. Ferrari, A. Di Molfetta, B. Meyns, Exercise physiology with a left ventricular assist device: Analysis of heart-pump interaction with a computational simulator. *PLOS ONE* **12**, e0181879 (2017).
27. J. M. Cheng, C. A. den Uil, S. E. Hoeks, M. van der Ent, L. S. D. Jewbali, R. T. van Domburg, P. W. Serruys, Percutaneous left ventricular assist devices vs. intra-aortic balloon pump counterpulsation for treatment of cardiogenic shock: A meta-analysis of controlled trials. *Eur. Heart J.* **30**, 2102–2108 (2009).
28. K. D. Sjauw, A. E. Engström, M. M. Vis, R. J. van der Schaaf, J. Baan Jr., K. T. Koch, R. J. de Winter, J. J. Piek, J. G. P. Tijssen, J. P. S. Henriques, A systematic review and meta-analysis of intra-aortic balloon pump therapy in ST-elevation myocardial infarction: Should we change the guidelines? *Eur. Heart J.* **30**, 459–468 (2009).
29. H. Thiele, U. Zeymer, F.-J. Neumann, M. Ferenc, H.-G. Olbrich, J. Hausleiter, G. Richardt, M. Hennersdorf, K. Empen, G. Fuernau, S. Desch, I. Eitel, R. Hambrecht, J. Fuhrmann, M. Böhm, H. Ebelt, S. Schneider, G. Schuler, K. Werdan; IABP-SHOCK II Trial Investigators, Intraaortic balloon support for myocardial infarction with cardiogenic shock. *N. Engl. J. Med.* **367**, 1287–1296 (2012).
30. I. Parviainen, S. M. Jakob, M. Suistomaa, J. Takala; Scandinavian Society of Anaesthesiology and Intensive Care Medicine (SSAI), Practical sources of error in measuring pulmonary artery occlusion pressure: A study in participants of a special intensivist training program of The Scandinavian Society of Anaesthesiology and Intensive Care Medicine (SSAI). *Acta Anaesthesiol. Scand.* **50**, 600–603 (2006).
31. J. J. Ryan, J. D. Rich, T. Thiruvoipati, R. Swamy, G. H. Kim, S. Rich, Current practice for determining pulmonary capillary wedge pressure predisposes to serious errors in the classification of patients with pulmonary hypertension. *Am. Heart J.* **163**, 589–594 (2012).
32. Abiomed, *Impella CP—Instructions for Use & Clinical Reference Manual* (Abiomed, 2014).
33. B. J. E. Misgeld, D. Rüschen, S. Schwandtner, S. Heinke, M. Walter, S. Leonhardt, Robust decentralised control of a hydrodynamic human circulatory system simulator. *Biomed. Signal Process. Control* **20**, 35–44 (2015).
34. P. F. Watson, A. Petrie, Method agreement analysis: A review of correct methodology. *Theriogenology* **73**, 1167–1179 (2010).

Acknowledgments: We thank A. Spognardi and the team at CBSET Inc. for assistance in conducting the animal experiments, K. Feng and S. Russman for aid in data analysis and review of the manuscript, and A. Kalluri for advice regarding data analysis and review of the manuscript. **Funding:** E.R.E. was funded in part by NIH R01 GM49039. S.P.K. was funded by NIH 5T32EB016652-02. Funding and critical supplies were provided by Abiomed through an educational research grant awarded to B.Y.C. and E.R.E. **Author contributions:** B.Y.C. and E.R.E. conceptualized and designed the project. S.S.B. and N.J. provided technical details and support for Impella operation. B.Y.C. designed and conducted MCL experiments. All authors designed and conducted animal studies. B.Y.C. collated and analyzed MCL and animal study results. B.Y.C., S.P.K., and E.R.E. collected and analyzed retrospective patient data. B.Y.C., S.P.K., and E.R.E. wrote the manuscript. **Competing interests:** E.R.E., B.Y.C., N.J., and S.S.B. are co-inventors on pending U.S. patent 15/709,080 submitted by the Massachusetts Institute of Technology that covers extraction of hemodynamic metrics from MCS devices. S.S.B. and N.J. are employees of Abiomed. All other authors have no other conflict of interests. **Data and materials availability:** Additional information is available from the corresponding author on reasonable request.

Submitted 5 July 2017
Resubmitted 12 September 2017
Accepted 25 January 2018
Published 28 February 2018
10.1126/scitranslmed.aao2980

Citation: B. Y. Chang, S. P. Keller, S. S. Bhavsar, N. Josephy, E. R. Edelman, Mechanical circulatory support device-heart hysteretic interaction can predict left ventricular end diastolic pressure. *Sci. Transl. Med.* **10**, eaao2980 (2018).

Science Translational Medicine

Mechanical circulatory support device-heart hysteretic interaction can predict left ventricular end diastolic pressure

Brian Y. Chang, Steven P. Keller, Sonya S. Bhavsar, Noam Josephy and Elazer R. Edelman

Sci Transl Med **10**, eaao2980.
DOI: 10.1126/scitranslmed.aao2980

Predicting pressure from a pump

Mechanical ventricular assist devices help the heart pump blood after cardiac surgery or while awaiting heart transplant. Chang *et al*. show that the motor current and pressure head recorded by the Impella, a temporary assist device placed within the left ventricle, can be used to measure left ventricular end diastolic pressure (LVEDP). LVEDP indicates cardiac function and is used to titrate mechanical pump support. Chang and colleagues found that Impella-based LVEDPs matched left heart catheter-based LVEDPs more closely than pulmonary capillary wedge pressure–inferred LVEDPs. After testing in a mock circulatory loop and a pig model of cardiac dysfunction, they confirmed their findings with patient data. This method does not require any modification of the Impella assist device, suggesting that it could be easily adopted into clinical practice.